Results in Engineering 16 (2022) 100763

Contents lists available at ScienceDirect

Results in Engineering

journal homepage: www.sciencedirect.com/journal/results-in-engineering

The efficiency of CFRP strengthening and repair system on the flexural behavior of RC beams constructed with different concrete compressive strength

Meyyada Y. Alabdulhady *, Mohammed F. Ojaimi, Aqeel H. Chkheiwer

Department of Civil Engineering, University of Basrah, Basrah, Iraq

A R T I C L E I N F O

Keywords:
CFRP composite
Concrete compressive strength
Flexure strengthening
Moment
RC beams
Repair

A B S T R A C T

This paper presents experimental investigation on the effectiveness of CFRP strengthening and repair system on the load carrying capacity, stiffness, flexural behavior, and failure mode mechanism of RC beams constructed with different concrete compressive strength (f_c'). Eight RC simply supported beams were strengthened and repaired with one layer of CFRP composite and tested experimentally under flexural load. The beams were built with varying the concrete compressive strength (f_c') value of (21.1, 36.1, 48.2, and 68.5) MPa, to demonstrate low, normal, and high strength. The results obtained in this work revealed that the performance of the CFRP composite material was inversely correlated to the concrete compressive strength in repaired beams while a proportion relation was observed in strengthened beams only with low to normal concrete strength. Finally, reasonable agreement between the estimated bending moment capacities for strengthened beams (based on the ACI 440.2R-17 provision) and the experimental results within ±16% were obtained.

1. Introduction

In recent decades, there has been an increased attention to strengthening or/and rehabilitation of existing reinforced concrete structures in buildings and bridges. The need for strengthening and/or rehabilitation arises because of the change in codes requirements, changing in architectural layout that result in an increase in utilized loading, deterioration of internal reinforcement caused by weather, and damage of the concrete cover because of corrosion, fire, and aging of concrete, among other factors [1,2]. Furthermore, after an earthquake, damaged structure elements must be retrofitted to restore their original capacity [3,4]. As a result, many materials and products have been used to address these deficiencies, with a high degree of success. In comparison with the old approaches for strengthening such as steel jackets and/or concrete size enlargements, Fiber-Reinforced Polymer (FRP) is the repairing technique that has been demonstrated to be the most successful and reliable system [5]. Higher amount of tensile strength to the weight ratio; higher durability, non-corrosion, and longer efficient service life of FRP composite material contributes to its efficacy and strength [6].

Several experimental tests have been conducted on the impact of adding externally bonded FRP material to RC beams for flexural augmentation and improvement. In addition, researchers have focused their efforts on examining the effect of several parameters to assess the performance of the composite system by utilizing different fiber textiles or adjusting the composite configuration, changing number of plies, varying the reinforcing ratio, substrate surface preparation and uneven levels of damage severity were also considered in their studies [7–26]. For instant, Alagusundaramoorthy et al. [14] and Attari et al. [17] studied the effectiveness of adding different layouts of externally bonded CFRP sheets on increasing the flexural strength of concrete beams. Esfahani et al. [12] examined experimentally the effect of internal reinforcing ratio ρ on the flexural strength and behavior of the strengthened beams with considering the effect of varying the width, length, and number of layers of CFRP sheets. Al-Shamayleh et al. [27] presented experimentally and analytically the effectiveness of two types of CFRP composites attached in six different configurations with three grades of concrete strength (17, 32, and 47) MPa. The results showed the effectiveness of the CFRP composite material was inversely proportional to the concrete strength. In case of repairing RC beams, Benjeddou et al. [13] experimental study was conducted on repairing damaged RC beams with CFRP composite. Beams were constructed with two types of

* Corresponding author.
E-mail address: meyyada.yahya@uobasrah.edu.iq (M.Y. Alabdulhady).

https://doi.org/10.1016/j.rineng.2022.100763
Received 18 September 2022; Received in revised form 7 November 2022; Accepted 9 November 2022
Available online 11 November 2022

concrete strength C21 and C38 and repaired using different amounts of CFRP laminates with considering the influences of changing different parameters such as the damage degree and the CFRP laminate width. The results revealed that, for any concrete type, the CFRP composite added about a half of the load capacity. Fayyadh and Razak [19] investigated experimentally the effectiveness of adding CFRP sheets as a repaired material for RC beams with different levels of damage severity. It is obvious from the available literature that the efficiency and effectiveness of CFRP strengthening and repair system on the flexural behavior of RC beams constructed with different concrete compressive strength ($f_c^{'}$) has not yet been explored intensively. A very few studies addressed the impact of concrete compressive strength on the strengthening and retrofitting of reinforced concrete members [8, 27–30], therefore, more investigation needs to be considered for better understanding on such impact.

The goal of this study is to examine and evaluate the effectiveness of CFRP strengthening and repair system on the load carrying capacity, stiffness, flexural behavior, and failure mode mechanism of RC beams constructed with different concrete compressive strength ($f_c^{'}$). Eight RC beams are strengthened and repaired with one layer of CFRP composite system. Concrete compressive strength is varied from low strength (21.1 MPa) to normal (36.1 MPa) and high strength (48.2 and 68.5) MPa. Furthermore, a comparison of load-deflection behavior between strengthened and repaired beams separately with different concrete compressive strengths are presented and discussed. The estimation of ultimate moment capacity of strengthened beams by using ACI 440.2R-17 provision is also examined.

2. Experimental campaign

2.1. Specimens and materials

Eight RC beams were cast with four different values of concrete compressive strengths (low, normal, and high strength) (i.e., 21.1, 36.1, 48.2, and 68.5) MPa. The rules of the ACI 318 code [31] were employed to design the under-investigated beams. All beams had the same dimensions with (200, 250 and 1700) mm, for (width, depth, and length) respectively as shown in Fig. 1. The concrete cover was 30 mm in all directions. The beams also had the same internal reinforcement details, S420 deformed bars were used for both longitudinal and transverse reinforcements, (2φ12 mm at top and bottom as a longitudinal reinforcement, and 10 mm bar at 80 mm as a transverse reinforcement). The ratios of internal reinforcement were 1.03% and 1.6% for flexural and shear respectively. The mechanical properties of steel reinforcement were obtained from the average of three coupon samples that were tested according to ASTM A370 [32] and the results are listed in Table 2.

Beams were classified into four series according to the concrete compressive strength (C:21, C:36, C:48 and C:68). Concrete mixture proportions for all series are listed in Table 1. For each series, concrete compressive strength was determined as the average of three 150 mm cubes according to BS EN 12390–3:2009 [33], while splitting tensile strength of each group was obtained from the average of three cylinders with dimension of (diameter:150 mm, length: 300 mm) according to ASTM C496M [34]. All specimens in this campaign (beams, cubes, and cylinders) were casted at the same time and cured in the same manner by covering all the specimens with damp burlap. The curing lasted for several days based on the compressive strength gained with considering reaching to 70% of the required compressive strength. Then all specimens kept together under the same conditions in the lab until the testing day. The properties of the concrete are summarized in Table 3 and all the required tests for the mechanical properties of internal reinforcement and concrete are shown in Fig. 2.

Each series consist of two beams, one as a control, and the other strengthened by using one layer of CFRP composite installed on the tension zone. To elucidate repairing, the control beams were tested until failure and then repaired with one layer of CFRP composite as in the strengthened beams. The designation of each series is tabulated in Table 4.

Ordinary Portland Cement Type I was used in all mixes, which is complied with the requirements of ASTM C150M [35]. Natural fine and coarse aggregates were utilized with specific gravity of 2.63 and 2.66 and water absorption of (1.2 and 0.67) % for fine and coarse aggregate, respectively. The requirements for grading and quality of the fine and coarse aggregate were based on ASTM C33M [36] with aggregate maximum size of 20 mm. To produce a high strength concrete with low water cement ratio and to control the workability, a third generation of superplasticizer (Sika ViscoCrete-180 GS [37]) based on Polycarboxylate polymers was used. Sika ViscoCrete-180 GS is a powerful superplasticizer which acts through several different mechanisms including surface adsorption resulting in improved flow, placing and compaction characteristics [37]. Tap water was used for preparing, casting, and curing regimes.

2.2. CFRP composite material

The CFRP composite used in this study consists of carbon fabric and

Table 1
Concrete mixture proportions.

Material (kg/m^3)	Quantity			
	C:21	C:36	C:48	C:68
Cement Type I	300.0	402.0	447.0	548.0
Coarse Aggregate	1113.5	1085.5	1068.0	1008.0
Fine Aggregate	782.5	723.5	710.5	674.0
Water	204.0	189.0	170.0	164.5
Super Plasticizer	–	2.15	5.15	6.85

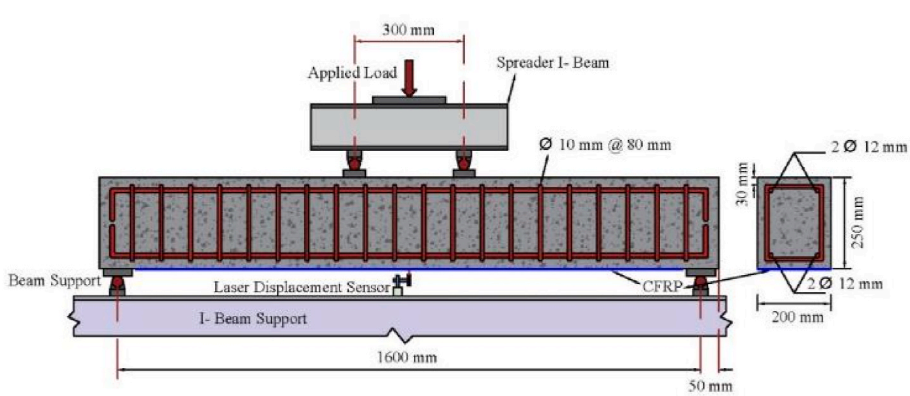

Fig. 1. Beams dimensions and reinforcement details.

Table 2
Measured mechanical properties of internal reinforcement.

Bar diameter (mm)	φ 10			φ 12		
Sample No.	1	2	3	1	2	3
Yield Stress, MPa	488	493	490	549	554	550
Standard deviation of yield stress, MPa		2.52			2.65	
Yield Stress, avg., MPa		490			551	
Ultimate strength, MPa	634	639	631	640	643	642
Standard deviation of ultimate strength, MPa		4.04			1.53	
Ultimate strength, avg., MPa		635			640	
Elongation, %	19	19	18.4	20	19.2	19.5
Elongation, avg., %		18.8			19.6	
Modulus of elasticity, GPa	196	204	199	202	198	201
Modulus of elasticity, avg., GPa		200			200	

Table 4
Beams designation.

Compressive strength, MPa	Beam description	Beam Designation
C:21	Control	A1
	Strengthened	A2
	Repaired	A3
C:36	Control	B1
	Strengthened	B2
	Repaired	B3
C:48	Control	C1
	Strengthened	C2
	Repaired	C3
C:68	Control	D1
	Strengthened	D2
	Repaired	D3

Table 3
Measured mechanical properties of concrete.

Material	Concrete			
	C:21	C:36	C:48	C:68
Compressive strength, MPa	21.1	36.1	48.2	68.5
Splitting tensile strength, MPa	1.70	2.46	3.10	4.29

epoxy agent. The carbon fabric was SikaWrap®-300C [38] which is a unidirectional woven fiber shown in Fig. 3, with the manufactural properties listed in Table 5. The adhesive agent that is used for attaching the carbon fibric sheet to the concrete substrate was Sikadur®-330 epoxy [39]. The epoxy agent consists of two-component which are thixotropic epoxy-based impregnating resin and adhesive which is used for attaching the carbon fabric sheet to the concrete substrate. The mechanical properties of the epoxy adhesive, Sikadur®-330, based on the datasheet provided by the supplier are listed in Table 6.

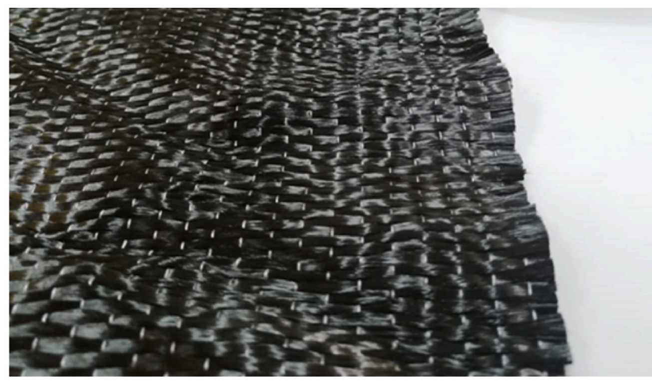

Fig. 3. Carbon fabric.

2.3. Strengthening and repair procedure

The strengthening and repair procedures that were followed in this work are summarized below and illustrated in Fig. 4:

1. For each beam, the Carbon fabric was cut into the desired length and width (i.e., 200 × 1500) mm.
2. To ensure a good bond between concrete and CFRP system, a grinder was used to roughen the tension surface of the beam, the lower face of the beam.

Table 5
Properties of carbon fiber (SikaWrap®-300 C).

Dry fiber density (g/cm^3)	Dry fiber thickness (mm)	Dry fiber tensile strength (MPa)	Dry fiber modulus of elasticity in tension (GPa)	Dry fiber elongation at break (%)
1.82	0.167	4000	230	1.7

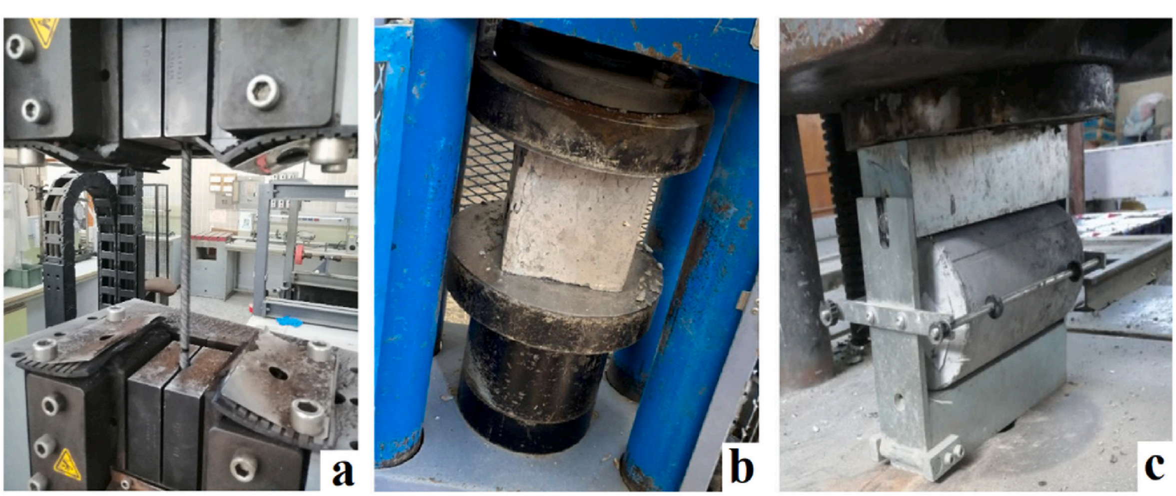

Fig. 2. Mechanical properties tests for a) rebar tensile strength b) concrete compressive strength c) splitting tensile strength.

Table 6
Properties of epoxy resin (Sikadur®-330).

Modulus of elasticity in flexure (MPa)	Tensile strength (MPa)	Modulus of elasticity in tension (MPa)	Tensile adhesion strength (MPa)	Elongation at break (%)
3800	30	4500	> 4	0.9

3. An air blower was used to remove all dust and dirt in order to clean the roughened surface.
4. The two epoxy agents were mixed properly by following the instruction in Sikadur®-330 datasheet [38]. For each beam, a thin layer of prepared epoxy agent was applied on the tension surface.
5. A dry method was used to install the strengthening system. The dry fabric was fixed on the fresh epoxy layer by pressing with hand first then with a roller to ensure the fabric is fully impregnated with a resin.
6. For repaired beams, all the damaged concrete parts of the tested control beams for all series were removed and the surface was cleaned from any dust or loose material. In this procedure, Sikalatex [40] which is a water-resistant bonding agent and mortar admixture with manufacture properties listed in Table 7, was used as a replacement of all the damaged concrete parts and sealing the cracks. The mix and application process of Sikalatex as a repair mortar was followed as mentioned in the data sheet [40]. Sikalatex was blended with the same portion of water and then added to a dry mix of cement and sand, mixed well then applied on the concrete surface. The repaired beams were left seven days for curing of the repair mortar before steps 2 to 5 were followed. The repair sequence is shown in Fig. 5. All beams (strengthened and repaired) were left at least seven

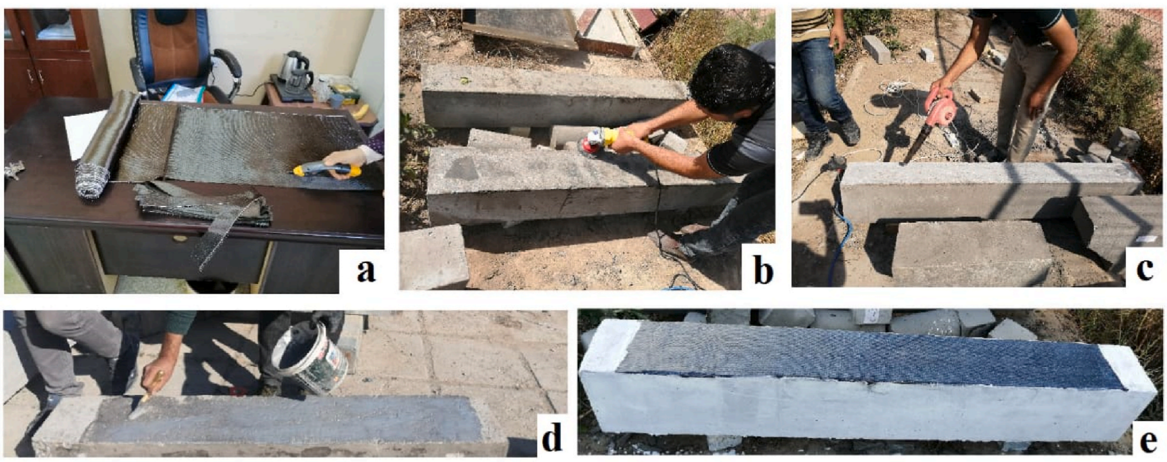

Fig. 4. Composite installation procedure for strengthened beams a) cutting the fabric b) roughen the tension surface c) surface cleaning d) applying the epoxy resin then the fabric e) finished surface.

Fig. 5. Repair procedure a) blending the Sikalatex with water b) mixing cement and sand with the wet part c) applying the repair mortar on the damaged area d) flatten and roughen the tension surface e) applying the epoxy resin then the fabric.

days at the room temperature, according to the manufacturer's instruction [39], for curing and hardening the epoxy resin before testing.

Table 7
Properties of Sikalatex.

Compressive strength (MPa)	Flexural strength (MPa)	Bond Strength (MPa)
35	6.5	1.5

2.4. Test setup and loading protocol

The beams under investigation were subjected to four-point bending test. The details and the locations of the four points loads are illustrated in Fig. 6. To apply the load on the specimens, a Universal Testing Machine (UTM) with a maximum load capacity of 500 kN was used. The beams were considered as simply supported with clear space of 1600 mm between the supports (Fig. 6). Midspan deflection was measured by using a digital laser dial indicator which is more accurate than the other gauges for precise reading. A load control protocol was performed with a constant load increment of 5 kN per min until the failure of the specimen. When the first crack occurred, the load was suspended for few seconds to label the cracks and to take pictures.

3. Experimental results

3.1. Load-deflection response

Fig. 7 shows the experimental relationship between applied load and mid-span deflection curves for the tested beams. The summary of experimental results is listed in Table 8. The test results in Table 8 includes the ultimate applied load P_u which is the largest load (the ultimate) was carried by the beams and corresponding deflection Δ_u which measured at beam midspan. The overall behavior of control beam in each series exhibited the same trend. This behavior can be divided into three phases. The elastic behavior phase characterized by a linear trend until the first crack initiated from the tension zone (the lower face of the beam) occurred. Then the second phase described by a non-linear behavior phase with a reduction in the bending stiffness due to the cracked section of the beam. The last phase started with yielding of steel bars in the tension zone and ended with reaching to the maximum applied load (failure load). For the strengthened and repaired beams, the overall behavior (i.e., load-deflection response) was the same with the behavior of the control beam except for the last phase, the external CFRP system contribution engaged as an additional reinforcement for carrying the additional applied load with the internal reinforcement until failure.

The load deflection response of strengthened beams clearly showed the high impact of the CFRP composite system on the overall behavior in compare with the control beam for all series as illustrated in Fig. 7. The uncracked section had a stiffer behavior in compare with the stiffness of the control beam as well as the repaired beam in all series. The highest increased in the load carrying capacity was for beam B2 with concrete compressive strength of $f_c' = 36.1$ MPa. The improvement was up to 54.5% in compare with the control beam B1. Moreover, the contribution of the CFRP composite for the rest of the strengthened beams on the ultimate load was (50.0, 37.3 and 46.2) % for beams (A2, C2 and D2) respectively. The mode of failure of the strengthened beams had a major impact on the improvement of the ultimate load which will be discussed in the following section.

For repaired beams, the uncracked flexural stiffness trend and the overall behavior were the same in compare with the control beam in series with normal to high concrete compressive strength of $f_c' = (36.1$, 48.2 and 68.5) MPa, Fig. 7(b, c and d). A slight improvement in the ultimate load capacity up to (18.2, 9.8 and 11.6) % for beams (B3, C3 and D3) respectively. On the other hand, the repaired beam with low magnitude of concrete compressive strength of $f_c' = 21.1$ MPa, beam A3, Fig. 7a, exhibited the same uncracked stiffness tendency as the control beam whereas the ultimate load capacity was considerably improved up to 44.9%. This recovery in repaired beams indicating that adding CFRP composite system as external reinforcement was a successful technique on restoring the original capacity and adding extra strength. This elaboration was tangible in beam with low concrete compressive strength with improvement up to 44.9%, while the enhancement decreased as the concrete compressive strength increased.

The ultimate deflection Δ_u for repaired beam A3 with low concrete strength of $f_c' = 21.1$ MPa, increased by 20.2%, while the deflection for repaired beam with concrete strength of $f_c' = 36.1$ MPa remained unchanged (beam B3). On the other hand, beams with higher compressive strength of $f_c' = (48.2$ and 68.5) MPa, the ultimate deflection was decreased up to (33.2 and 22.4) % for beams (C3 and D3) respectively. Notify that, all strengthened beams suffered from high reduction in the ultimate deflection (i.e., 24.1, 54.5 and 31.8) % for beams (B2, C2, and D2) respectively, except for beam A2 which had higher deflection than the control beam. As a result of adding the CFRP composite as un extra flexural reinforcement for high strength concrete beams, the deflection noticeably decreased. This can be explained by the nature of the CFRP composite system which is a linear elastic behavior with a brittle failure that led to loss some of the ductility of the structure [41–43].

To examine the contribution of CFRP system as an external flexural reinforcement with the influence of varying the concrete compressive strength on the strengthening and repaired beams separately, the strengthening beams from each series were collected together in one graph which is illustrated in Fig. 8a and similarly with the repaired beams as shown in Fig. 8b. CFRP system was more efficient in strengthened beams than the repaired beams by improving the strength. The improvement was noticeable for the strengthened beam B2 with concrete compressive strength of 36.1 MPa while the increase in the ultimate capacity was less prominent for beams with higher concrete strength. This significant improvement in the capacity can be related to the failure mode (fiber ruptured governed the failure for beam B2 which

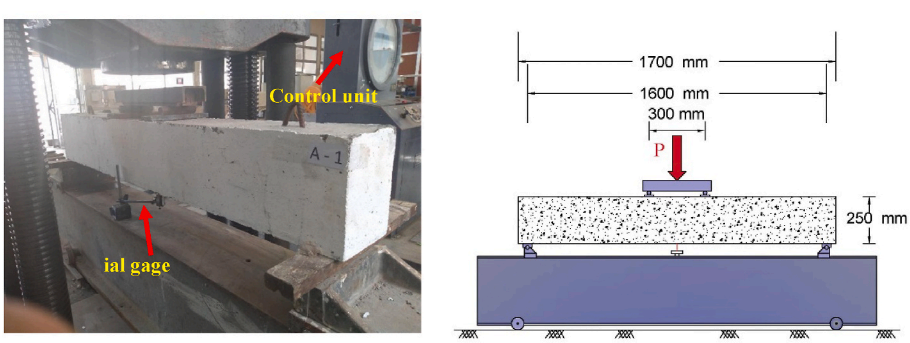

Fig. 6. Details of the test setup.

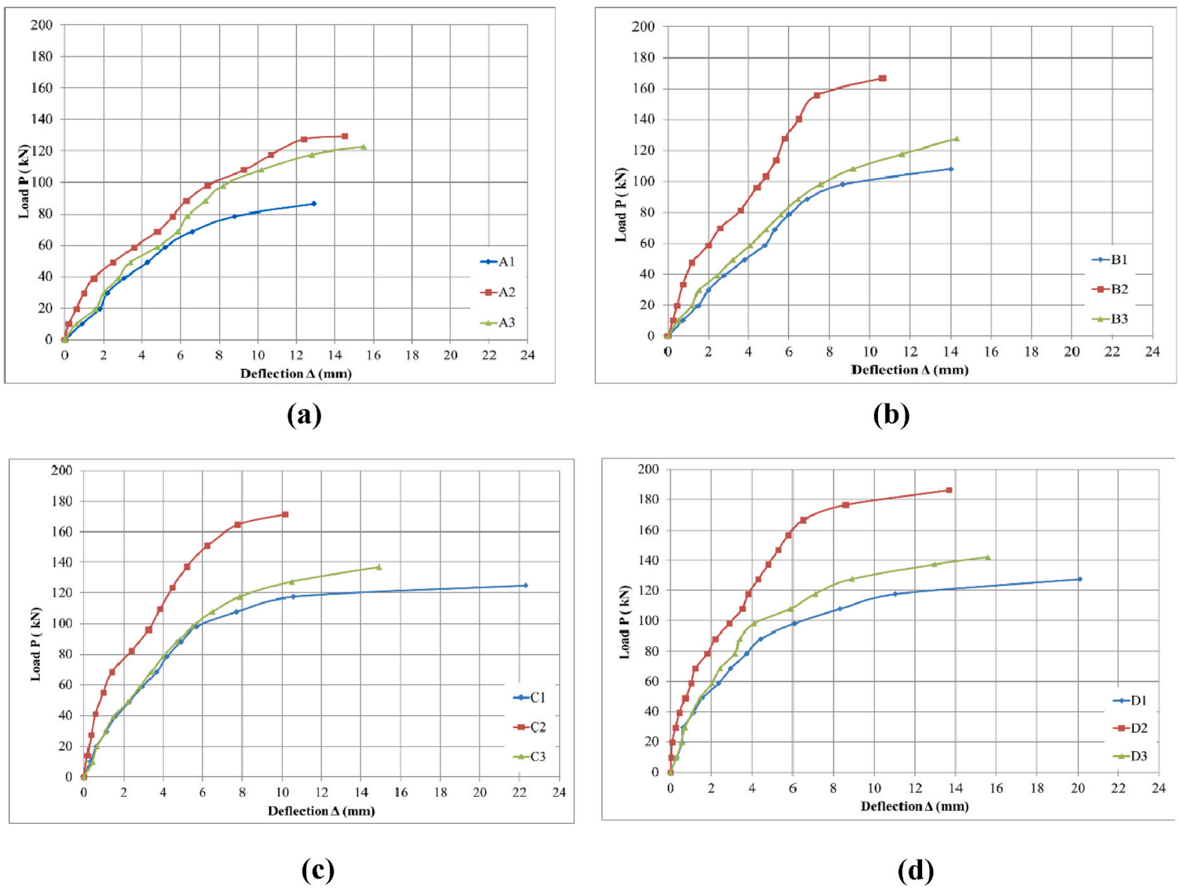

Fig. 7. Load deflection relationship.

Table 8
Summary of test results.

Beam	P_u (kN)	% Increase in P_u	Δ_u (mm)	% Change in Δ_u	Failure Modes
A1	86.3	–	12.9	–	Yielding of steel followed by concrete crushing
A2	129.4	50.0	14.5	12.4	Debonding
A3	122.6	44.9	15.5	20.2	Delamination
B1	107.9	–	14.0	–	Yielding of steel followed by concrete crushing
B2	166.7	54.5	10.62	−24.1	Yielding of steel followed by fiber rupture
B3	127.5	18.2	14.3	0.2	Debonding
C1	125.0	–	22.31	–	Yielding of steel followed by concrete crushing
C2	171.6	37.3	10.16	−54.5	Debonding
C3	137.3	9.8	14.9	−33.2	Debonding
D1	127.5	–	20.1	–	Yielding of steel followed by concrete crushing
D2	186.3	46.2	13.7	−31.8	Debonding
D3	142.2	11.6	15.6	−22.4	Yielding of steel followed by fiber rupture

will be discussed in the next section) or the value of concrete compressive strength of 36.1 MPa could be the saturation point for the current study. On the other hand, the repaired beams experienced a slightly improvement in the load carrying capacity as the concrete compressive strength increased (Fig. 8b). The overall behavior was nearly the same for all repaired beams. It should be noted that the performance of the CFRP composite material was inversely correlated to the concrete compressive strength in repaired beams while a proportion relation was observed in strengthened beams only with low to normal concrete strength.

3.2. Failure modes

Failure modes for control, strengthened and repaired beams are shown in Figs. 9–11 respectively. A closer shoot to different modes of failure is illustrated in Fig. 12. Control beams in all series (A1, B1, C1, and D1) were failed due to yielding of the internal steel reinforcement in the tension zone followed by crushing of concrete in the compression zone at beam mid-span. Vertical flexural cracks first formed between the two-points load at the beam mid-span then propagated towards the compression zone as the load increased. Moreover, flexural-shear cracks appeared close to the supports and then spread with inclination across the compression zone.

The strengthened beams in all series failed due to the debonding of the CFRP sheet near the support region (Fig. 12a) except for beam B2 which failed due to fiber ruptured located at the beam midspan (Fig. 12c). This failure was sudden and generated loud noise due to the

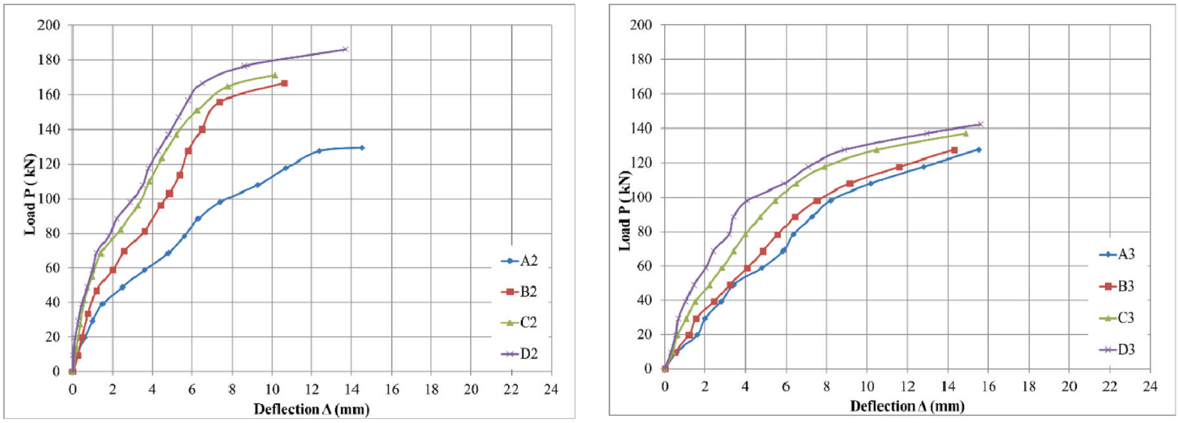

(a) (b)

Fig. 8. Load-deflection relationship comparison for a) strengthened beams b) repaired beams.

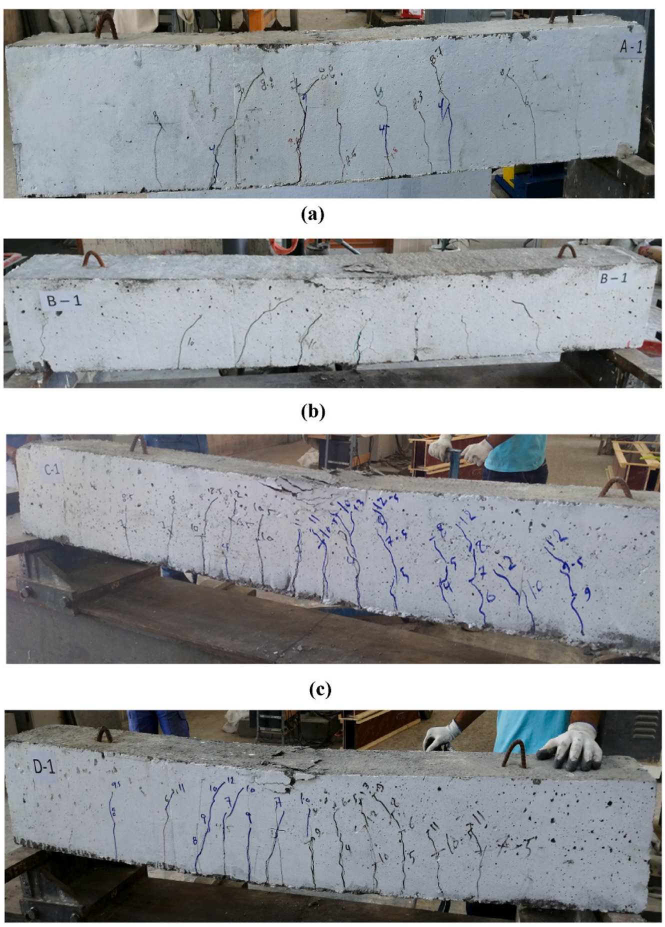

(a) (b) (c) (d)

Fig. 9. Failure modes of control beams for a) C:21 b) C:36 c) C:48 d) C:68.

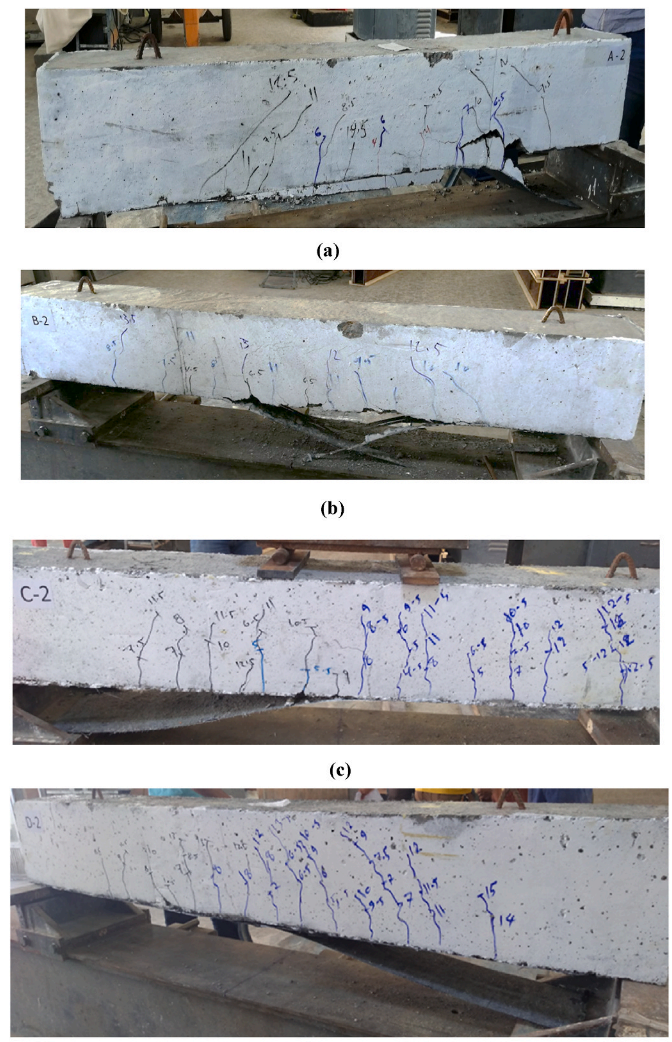

(a) (b) (c) (d)

Fig. 10. Failure modes of strengthened beams for a) C:21 b) C:36 c) C:48 d) C:68.

rapid release of energy that was hold by the composite. During the test, more cracks were spotted in compare with the cracks that formed in the control beam which were less and wider. That indicates, the CFRP composite helped to distribute the load throughout the entire tension surface with better usage of the composite as an external flexural reinforcement as well as arresting of the cracks that formed in the tension zone from widen and propagation.

Three different mode of failure was observed in the repaired beams. Delamination of the CFRP sheet with a thin layer of concrete cover was occurred in beam A3 (Fig. 12b), which is because of the low value of concrete compressive strength ($f_c' = 21.1$ MPa). While CFRP sheet was

(a)

(b)

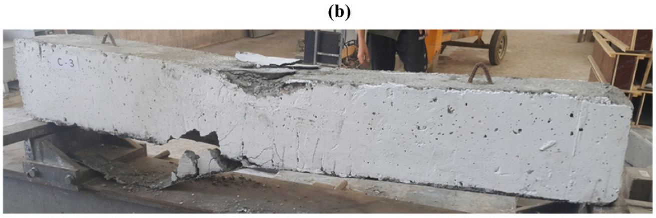

(c)

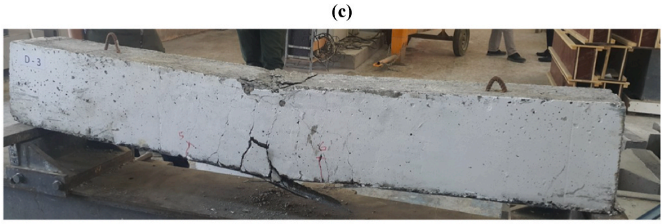

(d)

Fig. 11. Failure modes of repaired beams for a) C:21 b) C:36 c) C:48 d) C:68.

debonded without separating any of concrete cover near supports observed in beams B3 and C3 (Fig. 12a) which both had higher concrete compressive strength than beam A2. Beam D3 failed due to rupture of the fiber near the beam mid-span zone (Fig. 12c). Even though the failure mode of beam D3 which constructed with the highest concrete compressive strength ($f_c^{'}$ = 68.5 MPa) was due to fiber rupture, the improvement in the ultimate capacity was nearly as the value of beam C3 as shown in Fig. 8b. Therefore, the saturation point of concrete compressive strength for repaired beams in the current study could be $f_c^{'}$ = 48.2 MPa. However, more investigations are needed with concrete strength higher than 68.5 MPa to confirm the value of saturated point.

From the above observations and discussion, all strengthened and repaired beams failed due to debonding or delamination of the composite except for beam B2. In these failure modes, the full composite capacity was not reached and the precise relationship with the concrete compressive strength was not clear. Therefore, a suitable anchorage system is suggested to be used in further investigation to elaborat the composite with its full capacity by inducing fiber rupture failure mechanism.

4. Estimation of bending capacity for strengthened beams

In this section, the process of estimating the ultimate moment capacity for strengthened beams is presented and discussed. The ACI 440.2R-17 code provision guidance [44] was followed for the estimation. The nominal flexural strength is calculated based on the following equation according to Fig. 13:

$$M_n = A_s f_s \left(d - \frac{\beta_1 c}{2} \right) + A_f f_{fe} \left(d_f - \frac{\beta_1 c}{2} \right) \quad (1)$$

Where M_n is the nominal flexural strength (N.mm), A_s is the area of steel reinforcement (mm^2), f_s is the stress in steel reinforcement (MPa), d is the distance from extreme compression fiber to centroid of tension reinforcement (mm), c is the distance from extreme compression fiber to the neutral axis (mm), A_f is the area of FRP external reinforcement

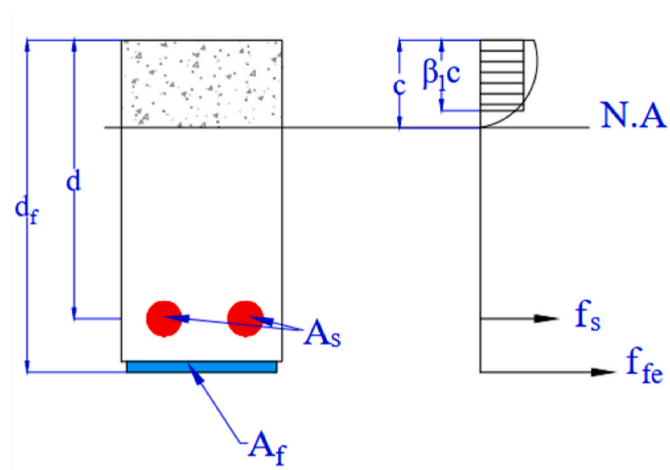

Fig. 13. Stress distribution over the section depth.

(a) (b) (c)

Fig. 12. Closer shoot for different mode of failure a) debonding b) cover delamination c) fiber rupture.

(mm^2), f_{fe} is the effective stress in the FRP (MPa), d_f is the effective depth of FRP flexural reinforcement (mm) and β_1 is the ratio of the depth of equivalent rectangular stress block to a depth of the neutral axis which depends on the concrete compressive strength. β_1 is 0.85 for concrete with $f_c^{'}$ is $\leq$ 27.6 MPa, and 0.05 less for each 6.9 MPa of $f_c^{'}$ greater than 27.6 MPa, however, β_1 should be not less than 0.65 as given in ACI 318 code [31].

In this study, all strengthened beams failed due to yielding in the internal reinforcement followed by the failure in the CFRP composite system either in debonding of the strips from the beam substrate or rupture of the fiber as discussed in previous section (Section 3.2). Therefore, the stress in the internal reinforcement is taken as the yield stress (f_y). The stress in the FRP is set to its effective stress as $f_{fe} = k_m f_{fu}$, where f_{fu} is the ultimate tensile strength of the CFRP material as reported by the manufacturer (MPa) [38], k_m is a bond-dependent coefficient which can be calculated using Eq. (2) below [45]:

$$k_m = \begin{cases} \frac{1}{60\varepsilon_{fu}}\left(1 - \frac{n.E_f.t_f}{360000}\right) \leq 0.90 \quad for\; n.E_f.t_f \leq 180000 \\ \frac{1}{60\varepsilon_{fu}}\left(\frac{90000}{n.E_f.t_f}\right) \leq 0.90 \quad for\; n.E_f.t_f > 180000 \end{cases} \tag{2}$$

Where n is the number of FRP plies, E_f is FRP tensile modulus of elasticity (MPa), t_f is one ply of FRP nominal thickness (mm).

The depth of the neutral axis c can be found from Equation (3) [46],

$$c = \frac{A_s f_y + A_f.k_m f_{fu}}{0.85 f_c^{'}.\beta_1.b} \tag{3}$$

Where $f_c^{'}$ is the concrete compressive strength (MPa) and b is the beam width (mm). The estimated value of the ultimate moment capacity ($M_{est.}$) of strengthened beams which was calculated based on the ACI 440.2R-17 [38], (Equation (1)), is compared to the experimental value ($M_{exp.}$). The estimated and experimental values are summarized in Table 9 and depicted in Fig. 14. The values of $M_{est.}$ are in reasonable agreement with those of $M_{exp.}$, within ±16%. In spite of the failure mode was governed by debonding of the majority of the strengthened beams (i.e., A2, C2 and D2) without reaching to the full capacity of the CFRP composite system, the estimation was acceptable in compare with the experimental results. The estimated value was higher than the experimental value for the beam with low concrete compressive strength ($f_c^{'}$ = 21.1 MPa, Beam A2) while for beams with higher concrete strength, the divergence in the results has increased significantly with under-estimating the value of ultimate moment capacity with up to (16%) for beam D2.

In addition to above explanation, it is notable that as the concrete compressive strength ($f_c^{'}$) increased up to (225%) in compare with the lower value of concrete strength ($f_c^{'}$ = 21.1 MPa), the increase in the bending moment capacity was only (12%) from the estimated calculations based on Equation (1). Whereas the experimental evidence showed a significant improvement in the ultimate moment capacity up to (44%) with an increase in the concrete compressive strength up to (225%). Based on the above results and according to ACI 440.2R-17 provision, the varying of concrete compressive strength may not be significantly have an impact on the ultimate moment capacity. It can be clearly concluded that the ACI 440.2R-17 approach is appropriate for estimating the ultimate moment capacity for strengthened beams with variation of concrete compressive strength between 30 and 70 MPa. However, more investigations are needed with wider range of values for the concrete compressive strength to support these findings.

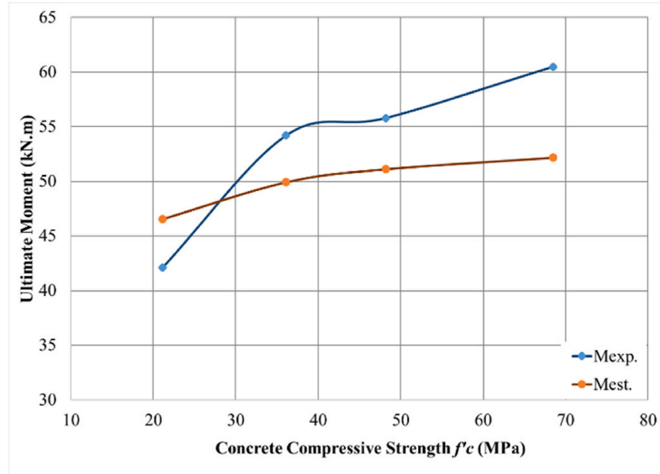

Fig. 14. Comparison between the experimental and estimated bending capacity with the varying of the concrete compressive strength.

5. Conclusions

In this study, the effectiveness of CFRP strengthening and repair system on the load carrying capacity, stiffness, flexural behavior, and failure mode mechanism of RC beams constructed with different concrete compressive strength ($f_c^{'}$) were examined. Eight RC beams were constructed with different concrete strength ($f_c^{'}$) (i.e., 21.1, 36.1, 48.2, and 68.5) MPa, (low, normal, and high strength) then strengthened and repaired with one layer of CFRP composite system to be evaluated experimentally under flexural load. The following significant conclusions were obtained:

1. For strengthened beams, beam B3 with $f_c^{'}$ = 36.1 MPa demonstrated a higher increase in the load carrying capacity (about 54.5%) in compare with the control beam B1, with fiber rupture governed the failure.
2. For repaired beams, beam A3 with low value of concrete compressive strength of $f_c^{'}$ = 21.1 MPa, showed the highest improvement in the ultimate load capacity (about 44.9%) in compare with the control beam A1, with composite delamination governed the failure.
3. Beams with low concrete compressive strength of $f_c^{'}$ = 21.1 MPa suffered from higher deflection than the control beam, while the deflection was less than or equal in the control beams for the rest of the strengthened and repaired beams in all series.
4. The performance of the CFRP composite material was inversely correlated to the concrete compressive strength in repaired beams while a proportion relation was observed in strengthened beams only with low to normal concrete strength.
5. Three failure modes were observed in this study: debonding of the composite from concrete substrate in beams (A2, B3, C2, C3, and

Table 9
The compared values between the experimental ($M_{exp.}$) and estimated ($M_{est.}$) bending capacity of the strengthened beams.

Beam	$f_c^{'}$ (MPa)	% Increase in $f_c^{'}$	*Mexp.* (kN.m)	% Increase in *Mexp.*	*Mest.* (kN.m)	% Increase in *Mest.*	*Mexp./Mest.*
A2	21.1	–	42.1	–	46.5	–	0.90
B2	36.1	71	54.2	29	49.9	7	1.09
C2	48.2	128	55.8	33	51.1	10	1.09
D2	68.5	225	60.5	44	52.2	12	1.16

D2), delamination of the composite with thin layer of concrete cover in beam A3, while beams B2 and D3 failed due to fiber rupture.
6. The saturation points of the concrete compressive strength in this study were (36.1 and 48.2) MPa for strengthened and repaired beams, respectively. However, more investigations are needed to confirm these results.
7. A reasonable agreement between the estimated bending moment capacity (based on the ACI 440.2R-17 provision) and the experimental results within was obtained, which was ±16%.
8. Finally, the ACI 440.2R-17 approach can be appropriate for estimating the ultimate moment capacity for strengthened beams with variation of concrete compressive strength between 30 and 70 MPa.

Credit author statement

Writing original draft was by Dr. Meyyada Y. Alabdulhady **Experimental investigation** was conducted by Dr. Aqeel H. Chkheiwer, Mr. Mohammed F. Ojaimi and Dr. Meyyada Y. Alabdulhad.

Declaration of competing interest

The authors declare that they have no known competing financial interests or personal relationships that could have appeared to influence the work reported in this paper.

Data availability

No data was used for the research described in the article.

References

[1] C.E. Bakis, L.C. Bank, V. Brown, E. Cosenza, J.F. Davalos, J.J. Lesko, T. C. Triantafillou, Fiber-reinforced polymer composites for construction-state-of-the-art review, J. Compos. Construct. 6 (2) (2002) 73–87.
[2] M.M. Rafi, A. Nadjai, F. Ali, D. Talamona, Aspects of behaviour of CFRP reinforced concrete beams in bending, Construct. Build. Mater. 22 (3) (2008) 277–285.
[3] H.S. Kim, Y.S. Shin, Flexural behavior of reinforced concrete (RC) beams retrofitted with hybrid fiber reinforced polymers (FRPs) under sustaining loads, Compos. Struct. 93 (2) (2011) 802–811.
[4] Y.T. Obaidat, S. Heyden, O. Dahlblom, G. Abu-Farsakh, Y. Abdel-Jawad, Retrofitting of reinforced concrete beams using composite laminates, Construct. Build. Mater. 25 (2) (2011) 591–597.
[5] F.W. Klaiber, K.F. Dunker, T.J. Wipf, W.W. Sanders Jr., Methods of strengthening existing highway bridges, Transport. Res. Rec. 1180 (1988) 1–6.
[6] N.F. Grace, G.A. Sayed, A.K. Soliman, K.R. Saleh, Strengthening reinforced concrete beams using fiber reinforced polymer (FRP) laminates, ACI Struct. J.-Am. Concr. Inst. 96 (5) (1999) 865–874.
[7] A. Nanni, Flexural behavior and design of RC members using FRP reinforcement, J. Struct. Eng. 119 (11) (1993) 3344–3359.
[8] N.F. Grace, G. Abdel-Sayed, W.F. Ragheb, Strengthening of concrete beams using innovative ductile fiber-reinforced polymer fabric, Struct. J. 99 (5) (2002) 692–700.
[9] P. Alagusundaramoorthy, I.E. Harik, C.C. Choo, Flexural behavior of R/C beams strengthened with carbon fiber reinforced polymer sheets or fabric, J. Compos. Construct. 7 (4) (2003) 292–301.
[10] L. Anania, A. Badalà, G. Failla, Increasing the flexural performance of RC beams strengthened with CFRP materials, Construct. Build. Mater. 19 (1) (2005) 55–61.
[11] H.A. Baky, U.A. Ebead, K.W. Neale, Flexural and interfacial behavior of FRP-strengthened reinforced concrete beams, J. Compos. Construct. 11 (6) (2007) 629–639.
[12] M.R. Esfahani, M.R. Kianoush, A.R. Tajari, Flexural behavior of reinforced concrete beams strengthened by CFRP sheets, Eng. Struct. 29 (10) (2007) 2428–2444.
[13] O. Benjeddou, M.B. Ouezdou, A. Bedday, Damaged RC beams repaired by bonding of CFRP laminates, Construct. Build. Mater. 21 (6) (2007) 1301–1310.
[14] R. Kotynia, H. Abdel Baky, K.W. Neale, U.A. Ebead, Flexural strengthening of RC beams with externally bonded CFRP systems: test results and 3D nonlinear FE analysis, J. Compos. Construct. 12 (2) (2008) 190–201.
[15] L. Li, Y. Guo, F. Liu, Test analysis for FRC beams strengthened with externally bonded FRP sheets, Construct. Build. Mater. 22 (3) (2008) 315–323.
[16] J. Dong, Q. Wang, D. He, Z. Guan, CFRP sheets for flexural strengthening of RC beams, in: 2011 International Conf*erence on Multimedia Technology*, 2011, pp. 1000–1003. July.
[17] N. Attari, S. Amziane, M. Chemrouk, Flexural strengthening of concrete beams using CFRP, GFRP and hybrid FRP sheets, Construct. Build. Mater. 37 (2012) 746–757.
[18] A. Balsamo, F. Nardone, I. Iovinella, F. Ceroni, M. Pecce, Flexural strengthening of concrete beams with EB-FRP, SRP and SRCM: experimental investigation. Composites Part B, Engineering 46 (2013) 91–101.
[19] M.M. Fayyadh, H.A. Razak, Analytical and experimental study on repair effectiveness of CFRP sheets for RC beams, J. Civ. Eng. Manag. 20 (1) (2014) 21–31.
[20] R. Reşatoğlu, M. Nasır Said, Behavior of reinforced concrete beams strengthened with CFRP, Am. Acad. Sch. Res. J. 7 (3) (2015).
[21] A. Saribiyik, N. Caglar, Flexural strengthening of RC beams with low-strength concrete using GFRP and CFRP, Struct. Eng. Mech. 58 (5) (2016) 825–845.
[22] P. Bodzak, Flexural behaviour of concrete beams reinforced with different grade steel and strengthened by CFRP strips, Compos. B Eng. 167 (2019) 411–421.
[23] M. Mashrei, J. Makki, A.A. Sultan, Flexural strengthening of reinforced concrete beams using carbon fiber reinforced polymer (CFRP) sheets with grooves, Lat. Am. J. Solid. Struct. 16 (2019).
[24] A.T. Obaidat, Flexural behavior of reinforced concrete beam using CFRP hybrid system, Eur. J. Environ. Civil Eng. (2021) 1–23.
[25] V.I. Fernandez-Davila, M.M. Gutierrez, J.D. Samaniego, J.L. Bazan, S.C. Santa-Cruz, Flexural behavior of reinforced concrete beams strengthened with composite carbon fiber-reinforced polymer system, ACI Struct. J. 119 (3) (2022).
[26] R.J. Abed, M.A. Mashrei, A.A. Sultan, Flexural behavior of reinforced concrete beams strengthened by carbon fiber reinforced polymer using different strengthening techniques, Adv. Struct. Eng. 25 (2) (2022) 355–373.
[27] R. Al-Shamayleh, H. Al-Saoud, M. Alqam, Shear and flexural strengthening of reinforced concrete beams with variable compressive strength values using externally bonded carbon fiber plates, Res. Eng. 14 (2022), 100427.
[28] H.K. Chinthapalli, M. Chellapandian, A. Agarwal, S.S. Prakash, Effectiveness of hybrid fibre-reinforced polymer retrofitting on behaviour of fire damaged RC columns under axial compression, Eng. Struct. 211 (2020), 110458.
[29] M.E. Abdel-Jaber, M.T. Abdel-Jaber, H. Katkhuda, N. Shatarat, R. El-Nimri, Influence of compressive strength of concrete on shear strengthening of reinforced concrete beams with near surface mounted carbon fiber-reinforced polymer, Buildings 11 (11) (2021) 563.
[30] J. Maheswaran, M. Chellapandian, N. Arunachelam, Retrofitting of severely damaged reinforced concrete members using fiber reinforced polymers: a comprehensive review (Elsevier), Structures 38 (2022) 1257–1276. April.
[31] ACI 318M-19, Building Code Requirements for Structural Concrete (318M-19) and Commentary (318R-19), American Concrete Institute, Farmington Hills, MI, 2019.
[32] ASTM A370-16, Standard Test Methods and Definitions for Mechanical Testing of Steel Products, ASTM International, West Conshohocken, PA, 2016, p. 49.
[33] B. En, 12390-3: 2009. Testing Hardened Concrete. Compressive Strength of Test Specimens, 2009, pp. 12390–12395.
[34] ASTM C496/C496M-11, Standard Test Method for Splitting Tensile Strength of Cylindrical Concrete Specimens, ASTM International, West Conshohocken, PA, 2011, p. 5.
[35] ASTM C150/C150M-18, Standard Specification for Portland Cement, ASTM International, West Conshohocken, PA, 2018, www.astm.org.
[36] ASTM C33/C33M-18, Standard Specification for Concrete Aggregates, ASTM International, West Conshohocken, PA, 2018, www.astm.org.
[37] Sika® ViscoCrete®-180 GS: High Range Water Reducing, Retarding and Slump Retaining Admixture. Product & Technical Data Sheet, Sika Company.
[38] SikaWrap 330C: Woven Carbon FIber Fabric for Structural Strengthening. Product & Technical Data Sheet, Sika Company.
[39] Sikadur 330: 2-part Epoxy Impregnation Resin. Product & Technical Data Sheet, Sika Company.
[40] Sikalatex: Water Resistant Bonding Agent and Mortar Admixture. Product & Technical Data Sheet, Sika Company.
[41] M. Masuelli (Ed.), Fiber Reinforced Polymers: the Technology Applied for Concrete Repair, BoD–Books on Demand, 2013.
[42] A. Nanni, A. De Luca, H. Jawaheri Zadeh, FRP Reinforced Concrete Structures–Theory, *Design And Practice* vol. 3, CRC Press, April, 2014, 400.
[43] V.P. Berardi, Fracture failure modes in fiber-reinforced polymer systems used for strengthening existing structures, Appl. Sci. 11 (14) (2021) 6344.
[44] ACI-440.2R, Guide for the Design and Construction of Externally Bonded FRP Systems for Strengthening Concrete Structures, American Concrete Institute, Farmington Hills, MI, USA, 2017.
[45] J.A. Barros, S.J. Dias, J.L. Lima, Efficacy of CFRP-based techniques for the flexural and shear strengthening of concrete beams, Cement Concr. Compos. 29 (3) (2007) 203–217.
[46] L.C. Bank, Composites for Construction: Structural Design with FRP Materials. Civil Engineering Journal, John Wiley & Sons, 2006.